THE JOURNAL OF BIOLOGICAL CHEMISTRY VOL. 288, NO. 27, pp. 19604–19613, July 5, 2013
© 2013 by The American Society for Biochemistry and Molecular Biology, Inc. Published in the U.S.A.

Identification and Functional Characterization of a Ku-binding Motif in Aprataxin Polynucleotide Kinase/Phosphatase-like Factor (APLF)*[S]

Received for publication, November 28, 2012, and in revised form, April 22, 2013 Published, JBC Papers in Press, May 20, 2013, DOI 10.1074/jbc.M112.440388

Purnata Shirodkar[‡§1], **Amanda L. Fenton**[‡§1], **Li Meng**[‡], **and C. Anne Koch**[‡§¶2]

From the [‡]*Ontario Cancer Institute, University Health Network, Toronto, Ontario M5G 2M9, Canada, the* [§]*Department of Medical Biophysics, University of Toronto, Toronto, Ontario M5G 2M9, Canada, and the* [¶]*Radiation Medicine Program, Princess Margaret Cancer Centre (University Health Network), Toronto, Ontario M5G 2M9, Canada*

Background: APLF interacts with Ku and facilitates nonhomologous end joining (NHEJ).
Results: APLF possesses a Ku-binding motif, and disruption of the APLF-Ku interaction impairs both NHEJ and the nuclear retention of APLF.
Conclusion: The APLF-Ku interaction is functionally important in DNA repair and may be important for APLF stability.
Significance: The APLF Ku-binding motif appears to represent a general Ku-binding motif.

Aprataxin polynucleotide kinase/phosphatase-like factor (APLF) facilitates nonhomologous end joining (NHEJ) and associates with the core NHEJ components XRCC4-DNA ligase IV and Ku. The APLF forkhead-associated (FHA) domain directs interactions with XRCC4, but the APLF-Ku interaction has not been well characterized. Here we describe an evolutionarily conserved amino acid motif within APLF that is required for mediating the physical interaction between APLF and Ku. This APLF Ku-binding motif possesses a similarity to regions identified in other NHEJ factors, WRN and XLF, which also direct interactions with Ku. Indeed, peptides derived from the Ku-binding region of APLF, WRN, or XLF were sufficient to reconstitute the interaction with Ku *in vitro*. Although APLF is localized predominantly to the nucleus, it does not possess a nuclear localization signal (NLS). Interestingly, the disruption of the APLF-Ku interaction by substituting key residues in the APLF Ku-binding motif was associated with increased relocalization of APLF to the cytoplasm and reduced association with XRCC4, which was rescued by the introduction of an NLS onto APLF. When human cells stably depleted of APLF were reconstituted with APLF Ku-binding mutants, or with an APLF FHA mutant that is known to disrupt interactions with XRCC4, APLF-dependent NHEJ and the retention of APLF at sites of laser-generated DNA damage were impaired. These data suggest functional requirements for Ku and XRCC4 in APLF-dependent NHEJ and a unique role for Ku as a factor required to facilitate the nuclear retention of APLF.

The DNA double strand break (DSB)[3] is widely believed to be the most deleterious and cytotoxic form of DNA damage (1, 2). Failure to resolve DSBs can give rise to the loss, amplification, rearrangement, or translocation of chromosomal material, thus leading to increased genomic instability and, consequently, an enhanced rate of carcinogenesis (3). In mammalian cells, NHEJ is the predominant repair mechanism for DSBs induced by exogenous factors such as IR and functions in all phases of the cell cycle (4).

The initial step in NHEJ involves the binding of Ku to the DSB ends. Ku, an abundant nuclear protein, is a very stable heterodimeric complex consisting of Ku70 (70 kDa) and Ku80 (80 kDa) (5, 6). The Ku70 and Ku80 subunits share sequence similarity in their N-terminal regions (the von Willebrand A and core domains), which are involved in heterodimerization (7). The C-terminal regions of Ku are divergent and, in the case of Ku80, direct the interactions with the DNA-dependent protein kinase catalytic subunit (DNA-PKcs) (6, 8).

The binding of Ku to DNA ends is thought to protect the ends from nucleolytic degradation, to align and maintain the ends in close proximity, and to recruit DNA-PKcs to the DSB, which results in the activation of its kinase function (7). During synapsis, the broken DNA ends remain accessible to DNA end processors, such as polynucleotide kinase/phosphatase (PNKP) and aprataxin (APTX), which act to modify non-complementary or damaged termini to make them amenable to religation. In addition, other factors may be required during NHEJ to repair specific subsets of DSBs including the Werner syndrome protein (WRN), which possesses helicase and 3′ to 5′ exonuclease activities (9, 10). WRN also interacts physically with Ku, which strongly stimulates WRN exonuclease activity on DNA ends (11). DNA end processing is followed by DNA end joining,

* This work was supported by Canadian Institutes of Health Research (CIHR) Operating Grant MOP-102691 (to C. A. K.).
[S] This article contains supplemental Figs. S1–S6.
[1] Both authors contributed equally to this work and were supported by the Terry Fox Foundation Strategic Training Initiative for Excellence in Radiation Research for the 21st Century (EIRR21) at CIHR and the Lawrence, Ila and William Gifford Scholarship Fund.
[2] To whom correspondence should be addressed: Radiation Medicine Program, Princess Margaret Cancer Centre (UHN), 610 University Ave., Toronto, Ontario M5G 2M9, Canada. Tel.: 416-946-4662; Fax: 416-946-2111; E-mail: anne.koch@rmp.uhn.on.ca.

[3] The abbreviations used are: DSB, double strand break; SSB, single strand break; NHEJ, nonhomologous end joining; DNA-PKcs, DNA-dependent protein kinase catalytic subunit; PNKP, polynucleotide kinase/phosphatase; APTX, aprataxin; XLF, XRCC4-like factor; APLF, APTX/PNKP-like factor; FHA, forkhead-associated; PBZ, poly(ADP-ribose)-binding zinc finger; NLS, nuclear localization signal; WCE, whole cell extract; WRN, Werner syndrome protein.

catalyzed by the XRCC4-DNA ligase IV complex. The nuclear phosphoprotein XRCC4 has weak intrinsic DNA binding capability, which is thought to be enhanced by interactions with Ku. Indeed, Ku has been shown to stimulate XRCC4-ligase IV end joining *in vitro* (12–14). Another core NHEJ protein, XRCC4-like factor (XLF, also known as Cernunnos), also co-associates with and stimulates the XRCC4-ligase IV complex to promote NHEJ (15, 16). Ku is required for the recruitment of XLF to DSBs, and XRCC4 promotes XLF accumulation at DSBs (17).

APTX/PNKP-like factor (APLF; also known as PALF and Xip1) is another DNA repair factor that participates in NHEJ and binds to Ku (18–20). APLF possesses an N-terminal FHA domain that mediates interactions with threonine-phosphorylated XRCC4 and XRCC1, a nuclear scaffold protein that participates in DNA single strand break (SSB) repair, which is analogous to XRCC4 (18–21). The APLF FHA domain is functionally similar to the FHA domains of PNKP and APTX, from which it derives its name (22–24). In addition to its FHA domain, APLF possesses two unique poly(ADP-ribose)-binding zinc finger (PBZ) domains in its C-terminal region, which direct interactions with poly(ADP-ribose) and are involved in the recruitment of APLF to sites of DNA damage (18, 19, 25–27). APLF accumulates at sites of SSBs or DSBs induced by DNA-damaging agents and is required for cellular resistance to a variety of DNA-damaging agents. We have also shown that APLF facilitates NHEJ and that APLF interacts with Ku, or with DNA-bound Ku, independently of the APLF FHA or PBZ domains (18, 19). APLF appears to lack intrinsic DNA binding ability, at least to linearized double-stranded DNA (18). Therefore, it is conceivable that Ku may facilitate the recruitment or retention APLF at DSBs *in vivo*.

APLF participates in DNA damage signaling and repair and has been shown to localize predominantly to the nucleus (18), but APLF has no identifiable nuclear localization signal (NLS). Passive nucleocytoplasmic translocation permits proteins smaller than ~60 kDa to diffuse through nuclear pore complexes in an energy-independent manner (28). In contrast, larger proteins cannot diffuse freely through nuclear pore complexes and are actively and selectively transported across the nuclear envelope (28, 29). Therefore, it is possible that APLF passively diffuses into the nucleus, as it is a small protein of 57 kDa.

To further delineate the role of APLF in NHEJ, and to better understand the functional importance of the APLF-Ku interaction in this process, we have identified and characterized the APLF Ku-binding motif. We show that the interaction with Ku appears to support the nuclear retention of APLF, and this interaction is required for the association with XRCC4-ligase IV. Collectively the data suggest that the interactions among APLF, Ku, and XRCC4 are important for APLF-dependent NHEJ and the accumulation of APLF at sites of DNA damage.

EXPERIMENTAL PROCEDURES

Cloning and Plasmid Constructions—To generate pcDNA3.1-V5/His-APLF$^{\Delta 180-200}$ (V5-APLF$^{\Delta 180-200}$), QuikChange site-directed mutagenesis (Stratagene) was used to remove amino acid residues 180–200 from pcDNA3.1-V5/His-APLF (18). QuikChange site-directed mutagenesis was also used to create the R182A, R184A, R182A/R184A, W189A, M190A, L191A, and W189A/M190A/L191A substitutions within pcDNA3.1-V5/His-APLF. To generate pcDNA3.1-V5/His-NLS-APLF, pcDNA3.1-V5/His-NLS-APLF$^{\Delta 180-200}$ and pcDNA3.1-V5/His-APLF^{W189A}, the SV40 large T-antigen nuclear localization signal (MAPKKKRKV) was inserted before the APLF sequence by QuikChange site-directed mutagenesis of the appropriate pcDNA3.1-V5/His-APLF construct. pcDNA3.1-V5/His-APLF was digested with BamHI and XhoI and ligated in-frame into pcDNA 3.1-Zeo-HA2.B (Invitrogen) to generate pcDNA 3.1-Zeo-HA2.B-APLF. To then generate pcDNA 3.1-Zeo-HA2.B-APLF$^{1-160}$, pcDNA 3.1-Zeo-HA2.B-APLF$^{1-180}$, and pcDNA 3.1-Zeo-HA2.B-APLF$^{1-200}$ (HA-APLF$^{1-160}$, HA-APLF$^{1-180}$, and HA-APLF$^{1-200}$), a stop codon was inserted by QuikChange site-directed mutagenesis after amino acid residues 160, 180, and 200, respectively, within pcDNA 3.1-Zeo-HA2.B-APLF. The pSUPER.retro.neo+GFP plasmid was used to express the APLF RNAi sequence GAAGAAATCTGCAAAGATA. A pSUPER RNAi-resistant APLF rescue construct harboring six different nucleotides in the RNAi target sequence GAG-GAGATTTGTAAGGAC (changed nucleotides are underlined) was generated by QuikChange site-directed mutagenesis. QuikChange site-directed mutagenesis was then used to create the following pSUPER RNAi-resistant APLF mutants using RNAi-resistant WT APLF as a template: R27A, W189A, NLS-W189A, R27A/W189A, R182A, R184A, M190A, L191A, NLS-APLF$^{1-200}$, and APLF^{ZF1+2m} (27).

The sequences encoding for the human *Ku80* open reading frame were PCR-amplified from the human cDNA IMAGE clone ID 4555162 (Open Biosystems) and TOPO-cloned in-frame into the EcoRI site of p3XFLAG-CMV-14 (Sigma) to generate p3XFLAG-CMV-14-Ku80 (3xFlag-Ku80). The human *Ku80* open reading frame was excised from p3XFLAG-CMV-14-Ku80 using EcoRI, cloned into the EcoRI site of pGEX4T3 (Amersham Biosciences), and pulled in-frame by site-directed mutagenesis to generate pGEX4T3-Ku80 (GST-Ku80). pGEX4T3-Ku80 was digested with XhoI and BamHI and ligated in-frame into pEGFP-C1 (Clontech) to generate pEGFP-C1-Ku80 (eGFP-Ku80). To then generate pEGFP-C1-Ku80$^{1-569}$, a stop codon was inserted by mutagenesis after amino acid residue 569 within pEGFP-C1-Ku80. To generate pBABE-puro-eCFP, pECFP-C1 (Clontech) was digested with ApaLI and AflII, blunt-ended, and ligated in-frame into the EcoRI site of pBABE-puro (Clontech).

Human APTX was PCR-amplified from cDNA IMAGE clone ID 6042653 (purchased from Open Biosystems) and TOPO-cloned into the pcDNA3.1-V5/His vector to generate pcDNA3.1-V5/His-APTX (APTX-V5). The human PNKP pcDNA3.1-V5/His-PNK (PNKP-V5) plasmid was constructed as described previously (23). All of the plasmid constructs were verified by sequence analysis.

Cell Culture and Transfections—HEK293T and U2OS cell lines were cultured in Dulbecco's modified Eagle's medium (DMEM) supplemented with 10% fetal bovine serum (FBS) and antibiotics. CHO-K1, XRS-5, XRC-1, EMC-11, and XR-1 cell lines were cultured in Alpha α-modified Eagle's medium supplemented with 10% FBS and antibiotics. To stably knock down endogenous APLF, U2OS cells were transfected with 2 μg of

either empty pSUPER vector ($U2OS^{NT}$) or pSUPER vector encoding the APLF RNAi sequence ($U2OS^{KD}$) and then selected with 800 μg/ml G418 (Invitrogen). Clonal U2OS cell lines were isolated and then maintained in DMEM supplemented with 10% FBS and 200 μg/ml G418. All cell lines were grown at 37 °C with a humidified atmosphere containing 5% CO_2. Transient transfections were performed with the Effectene transfection kit (Qiagen) according to the manufacturer's instructions.

Antibodies—Commercial antibodies used in this study were from Serotec (XRCC4 and DNA ligase IV), Cedarlane (Ku80), Cell Signaling (Ku70), Invitrogen (V5), Upstate (HA), Santa Cruz Biotechnology (GFP), Sigma (anti-FLAG M2) and Abcam (tubulin). Secondary antibodies for immunoblotting were from Jackson ImmunoResearch (goat anti-mouse and goat anti-rabbit), and secondary antibodies for immunofluorescence microscopy (goat anti-mouse Alexa 488 and goat anti-rabbit Alexa 488 secondary antibody) were from Invitrogen.

Protein Expression and Purification—GST-APLF recombinant protein was produced in *Escherichia coli* BL21(DE3)/pLysS (Novagen). Transformed bacteria were grown to an A_{600} of 0.6, and expression was induced by the addition of 1 mM IPTG (Sigma) for 3 h at 37 °C. The bacteria were then pelleted by centrifugation, washed with PBS, and recentrifuged. For purification, the cell pellet was resuspended in extraction buffer (50 mM Tris-Hcl, pH 7.5, 150 mM NaCl, 1 mM DTT, 1% Triton X-100, 1× Complete protease inhibitor mixture (Roche Applied Science), and disrupted by sonication. They lysates were clarified by centrifugation at 16,000 × *g* at 4 °C for 20 min. The supernatant was collected and incubated with glutathione-Sepharose 4B beads (Amersham Biosciences) for 2 h at 4 °C with gentle mixing. The beads were then washed and the protein eluted with extraction buffer containing 20 mM glutathione. The glutathione was then removed, and the purified protein was exchanged into a suitable buffer through three sequential rounds of dialysis using Slide-A-Lyzer dialysis cassettes (Pierce). Unless otherwise specified, all chemicals were purchased from Sigma Aldrich.

Preparation of Cell Extracts, Immunoprecipitation, and Immunoblotting—Whole cell extract (WCE) preparation, immunoprecipitations, and immunoblotting were performed as described previously (23). When indicated, lysates were prepared in the presence of 50 μg/ml ethidium bromide (Invitrogen). For pulldown assays using GST fusion proteins, clarified WCEs were incubated with 1 μg of the indicated GST fusion protein immobilized on glutathione-Sepharose 4B beads. The complexes were washed three times with lysis buffer and resuspended in sample buffer. For peptide pulldown assays, Dynabeads M-270 streptavidin (Invitrogen) was incubated with 50 ng of biotinylated peptide as indicated for 30 min at room temperature. The immobilized peptide beads (synthesized by Keck Biotechnology Resource Laboratory) were washed three times with PBS on a magnet and then mixed with 200 ng of purified recombinant Ku heterodimer (Trevigen) and incubated at 4 °C for 1 h. The beads were washed three times with PBS and resuspended with sample buffer. All peptides were synthesized with a linker consisting of two glycine residues between the biotin group and N terminus of the given peptide sequence and two C-terminal lysine residues to enhance solubility. Peptide sequences of the indicated proteins are underlined: $APLF^{WT}$, GGRKRILPTWMLKK; $APLF^{R184A}$, GGRKAILPTWMLKK; XLF, GGKRKKPRGLFSKK; and WRN, GGRKRRLPVWFAKK.

Random Plasmid Integration Assay—The random plasmid integration assay was performed essentially as described (15, 18) with some modifications. U2OS cells stably depleted in APLF were transfected with pSUPER RNAi-resistant APLF (wild type or mutants as indicated) or empty vector and incubated for 48 h at 37 °C. Subsequently, cells were transfected with linearized pBABE-puro-eCFP plasmid DNA. Twenty-four hours later, cells were replated at low density in selective media containing 2 μg/ml puromycin and incubated for 10 days at 37 °C. Colonies were then stained with Coomassie Blue dye and counted. A fraction of the transfected cells was monitored for nuclear eCFP expression to normalize the data for transfection efficiency. The relative plasmid integration of the APLF-depleted cell line reconstituted with RNAi-resistant $APLF^{WT}$ was set at 100% integration.

Immunofluorescence Microscopy—All procedures were performed at room temperature, solutions were prepared in PBS, and washes were performed between each step. For fixation, cells were incubated with 4% paraformaldehyde for 10 min. For immunostaining, cells were permeabilized by incubation with 0.5% Triton X-100 (Sigma) and 3% BSA (Sigma) for 10 min, blocked with 1.5% normal goat serum (Sigma) for 1 h, incubated with the indicated antibody for 2 h, and then incubated with secondary antibody for 1 h. Coverslips were then mounted on slides with Vectashield containing DAPI nucleic stain (Vector Laboratories). Slides were examined using a Zeiss AxioObserver microscope with a Plan-Neofluar ×40 objective. Image captured was achieved using a Roper Scientific CoolSnap HQ CCD camera. For subcellular localization analyses, 100 cells for each condition were analyzed in three independent experiments. Images were obtained using ImageJ and were adjusted for brightness and contrast only.

RESULTS

An Evolutionarily Conserved Region within APLF Is Required for Interaction with Ku—Our previous studies suggest that APLF amino acid residues 100–263, which are located between the FHA and PBZ domains, are sufficient for the association with Ku (18). In addition, it has been reported that APLF interacts directly with Ku80, suggesting that the Ku70/80 heterodimer interacts with APLF via Ku80 (19, 20). Within this region spanning APLF amino acid residues 100–263, residues 182–191 are highly conserved among APLF vertebrate homologues (Fig. 1*A*). We hypothesized that these conserved residues might be important for Ku binding and sought to further delineate the APLF-Ku binding region. To do so, we generated HA-tagged APLF C-terminal truncation peptides that were expressed in human HEK293T cells and examined them for their association with Ku in co-immunoprecipitation studies. We found that the APLF peptide containing the first 200 amino acid residues interacted well with Ku (monitored by anti-Ku80 immunoblotting), but no interaction was detected between Ku80 and the APLF peptides containing residues 1–160 or 1–180 (Fig. 1*B*). Similarly, an internal deletion of APLF residues

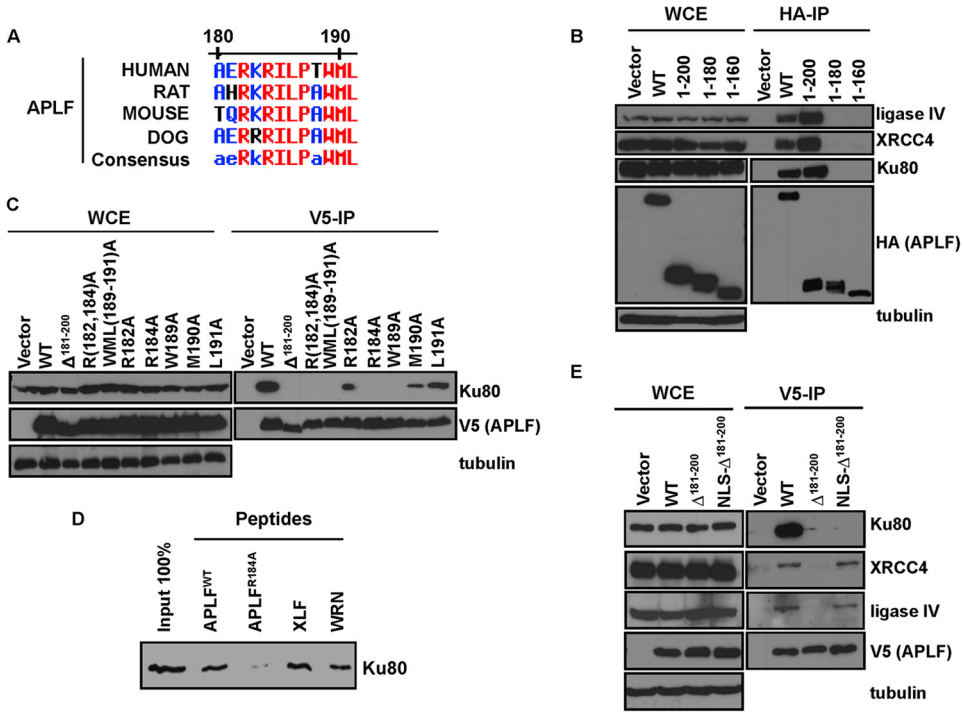

FIGURE 1. **Identification of a Ku-binding motif in APLF.** *A*, alignment (MultAlin) of human APLF and selected homologues. Invariant residues are identified by *red text*, and residues with greater than 50% consensus are identified by *blue text*. *B*, WCEs from HEK293T cells ectopically transfected with empty vector, HA-APLF^{WT}, HA-APLF$^{1-200}$, HA-APLF$^{1-180}$, or HA-APLF$^{1-160}$ were immunoprecipitated (*HA-IP*) with anti-HA antibody and immunoblotted with antibodies as indicated. Tubulin was used as a loading control. *C*, WCEs from HEK293T cells ectopically transfected with empty vector, WT APLF-V5, APLF$^{\Delta180-200}$-V5, or V5-tagged APLF mutants harboring single (R182A, R184A, W189A, M190A, L191A) or combinations of amino acid substitutions (R182A/R184A, W189A/M190A/L191A) were immunoprecipitated with anti-V5 antibody and immunoblotted with antibodies as indicated. *D*, 50 ng of biotinylated WT- or R184A-APLF, XLF, and WRN peptides was immobilized to streptavidin-Dynabeads, examined for its association with 200 ng of purified Ku70/80 in pulldown assays, and immunoblotted with anti-Ku80 antibody. *E*, WCEs from HEK293T cells ectopically transfected with empty vector, WT APLF-V5, APLF$^{\Delta181-200}$-V5, or NLS-APLF$^{\Delta180-200}$-V5 were immunoprecipitated with anti-V5 antibody, and the resulting protein complexes were immunoblotted with Ku80, XRCC4, DNA ligase IV, V5, or tubulin antibodies as indicated.

181–200 (APLF$^{\Delta181-200}$-V5) reduced the interaction with Ku80 (Fig. 1*C*).

We then examined the effect of smaller mutations, substituting individual APLF residues within the Ku-binding region (alone and in combination) using site-directed mutagenesis. Several highly conserved APLF residues (Fig. 1*A*) were substituted to alanine (R182A, R184A, W189A, M190A, L191A), and these mutant APLF proteins were compared with WT APLF for their ability to co-immunoprecipitate with Ku80. As shown in Fig. 1*C*, the APLF double substitution of R182A/R184A as well as the triple substitution of W189A/M190A/L191A to alanine abolished the interaction of APLF with Ku80. There was also a reduction in the association of Ku80 with singly substituted residues in this region of APLF, R182A and M190A, whereas the substitution of Leu-191 to alanine (L191A) had very little effect on the interaction (Fig. 1*C*). When we examined the APLF single substitutions of Arg-184 or Trp-189 to alanine (R184A and W189A respectively), there was no detectable interaction with Ku80 observed, suggesting that these residues are critical for the interaction of APLF with Ku. Consistent with this notion, a peptide corresponding to this Ku-binding region of APLF was sufficient to reconstitute the interaction *in vitro* with purified Ku70/80 heterodimer, whereas the corresponding mutant peptide harboring a single substitution of Arg-184 to alanine severely impaired the interaction (Fig. 1*D*). In addition, peptide sequences spanning the Ku-binding regions of WRN and XLF, which have amino acid similarity to the Ku-binding motif of APLF, also bound Ku *in vitro* (Fig. 1*D*).

Impact of the Ku-binding Region of APLF on XRCC4-Ligase IV Interactions—We have shown previously that the disruption of the APLF FHA domain (APLF-R27A) does not affect the association with Ku in human cells (18), but it is not known whether the disruption of APLF-Ku binding might affect interactions with XRCC4-ligase IV. When we initially examined interactions between the Ku-binding mutants APLF$^{\Delta181-200}$-V5, HA-APLF$^{1-180}$ and HA-APLF$^{1-160}$ with XRCC4 and ligase IV, we found that XRCC4-ligase IV interactions were undetectable on immunoblotting (Fig. 1, *B* and *E*). However, further examination of these transfected U2OS cells clearly demonstrated that the subcellular distribution of the APLF Ku-binding mutant proteins was altered (Fig. 2, *A* and *B*). Specifically, these mutant APLF peptides appeared to have a pancellular distribution compared with the predominantly nuclear localization of WT-APLF or the truncated mutant protein HA-APLF$^{1-200}$ (Fig. 2*A*), which both retain the ability to bind to Ku and XRCC4-ligase IV (Fig. 1*B*). Interestingly, when an NLS was introduced to APLF$^{\Delta181-200}$-V5 (NLS-APLF$^{\Delta181-200}$-V5), both the nuclear localization and the association with XRCC4-ligase IV were restored, although APLF-Ku80 binding remained undetectable (Fig. 1*E*). Similarly, the APLF double substitution R182A/R184A (*DM*) and triple substitution W189A/M190A/L191A (*TM*) Ku-binding mutants also displayed

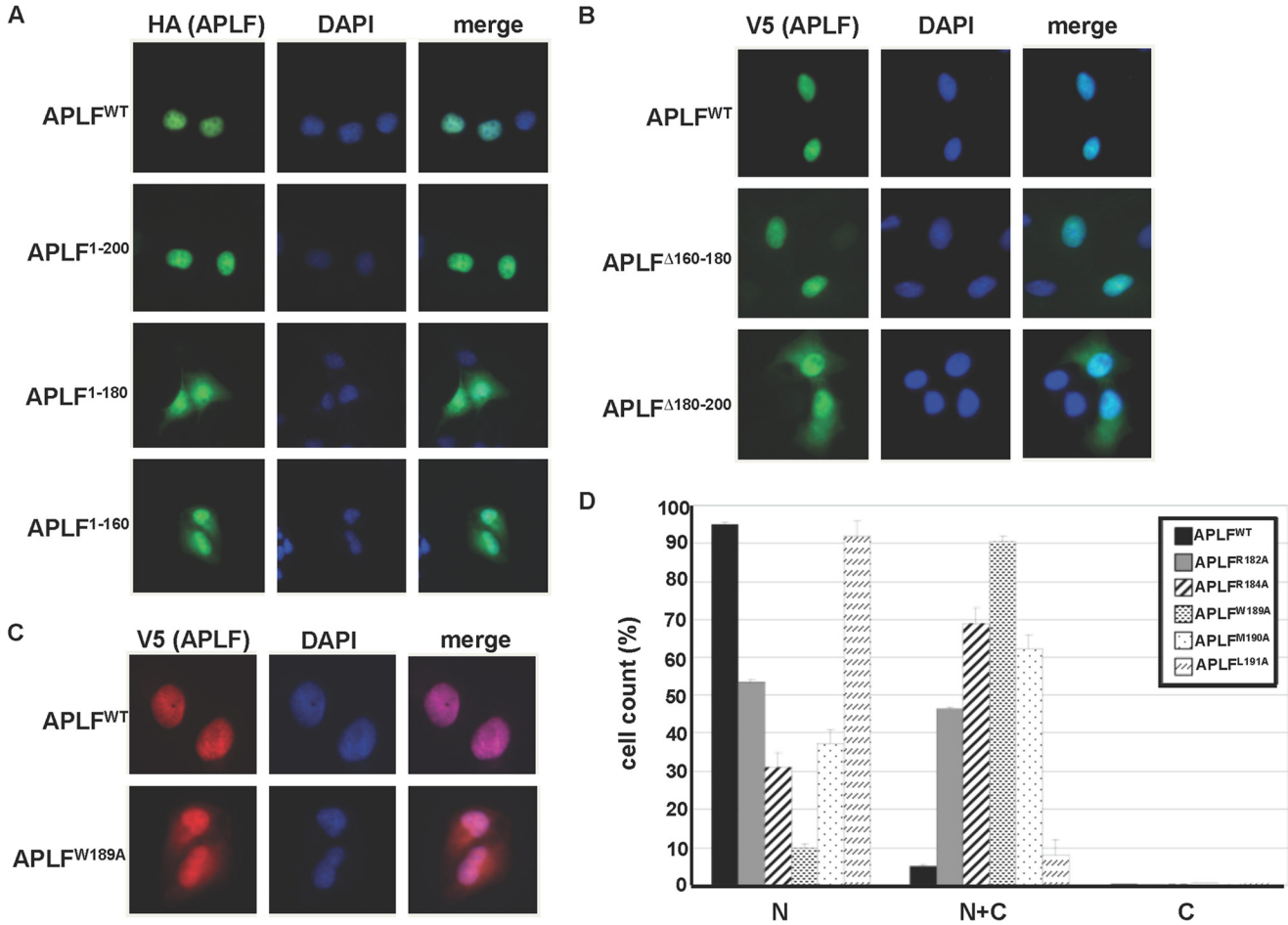

FIGURE 2. **Disruption of the APLF Ku-binding motif correlates with altered APLF subcellular localization.** U2OS cells ectopically expressing HA-tagged APLF^{WT}, APLF$^{1-200}$, APLF$^{1-180}$, or APLF$^{1-160}$ (*A*) or V5-tagged APLF^{WT}, APLF$^{\Delta160-180}$, or APLF$^{\Delta180-200}$ (*B*) were fixed and immunostained with anti-HA or anti-V5 antibodies as indicated. DAPI nuclear staining was merged with anti-APLF staining (*right panels*). *C*, U2OS cells stably depleted of APLF (U2OS^{KD}) ectopically expressing RNAi-resistant V5-tagged APLF^{WT} or APLF^{W189A} were fixed and immunostained with anti-V5 antibody and DAPI nuclear stain, and the images were merged (*right panel*). *D*, U2OS cells ectopically expressing V5-tagged WT APLF or APLF mutants harboring alanine substitutions (R182A, R184A, W189A, M190A, L191A) were fixed and immunostained with anti-V5 antibody, and the subcellular distribution (*N*, predominantly nuclear; *N*+*C*, pancellular; *C*, predominantly cytoplasmic) was quantified by immunofluorescence microscopy. Data represent the mean of 100 counted cells from three independent experiments, and *error bars* represent S.E.

impaired association with XRCC4 in co-immunoprecipitation studies (supplemental Fig. S1*A*). As reported previously (18), the observed interactions were not found to be affected by the presence of the DNA intercalating agent ethidium bromide, suggesting that the APLF-Ku and APLF-XRCC4 interactions are not bridged by DNA.

Disruption of the APLF-Ku Interaction Is Associated with Altered APLF Subcellular Localization in Mammalian Cells—To further examine the functional consequence of disrupting the APLF-Ku interaction on subcellular localization, we expressed one of the APLF mutants (W189A), which was found to have severely impaired association with Ku, in U2OS cells stably depleted of endogenous APLF. Consistent with the other defective Ku-binding APLF mutant cellular phenotypes, APLF^{W189A} also exhibited altered nuclear retention (Fig. 2*C*) as well as impaired association with XRCC4, which was restored by the addition of an NLS (NLS-W189A) (supplemental Fig. S1*B*). We then examined and quantified the subcellular distributions of WT APLF, or the APLF mutant proteins, R182A, R184A, M190A, and L191A, and found that the altered subcellular distribution of APLF appeared to correlate with defective Ku binding (Fig. 2*D*).

To ensure that these mutants were not simply disrupting the overall structure of the APLF protein and thereby affecting its subcellular localization, we next expressed WT APLF-V5 in CHO XRS-5 cells depleted of cellular Ku80 and therefore also deficient in Ku70 (Fig. 3). As a control, we also established that human WT APLF-V5 co-immunoprecipitated with hamster Ku80 and in reciprocal anti-Ku80 co-immunoprecipitations (Fig. 3*A*). Again, we noted that the predominantly nuclear localization of WT APLF-V5 was lost in the XRS-5 cells but not when it was expressed in the Ku-expressing CHO-K1 cells (Fig. 3*B*). The nuclear subcellular localization of APLF in XRS-5 cells was also restored when an NLS was engineered onto WT APLF-V5 (Fig. 3*B*). In contrast, U2OS cells stably depleted of APLF by shRNA (supplemental Fig. S1*C*) did not demonstrate altered Ku80 subcellular localization (supplemental Fig. S1*D*). We were not able to sufficiently deplete Ku80 from human cells to observe the phenotype under endogenous conditions with human APLF, as Ku is a very abundant nuclear protein. Lastly,

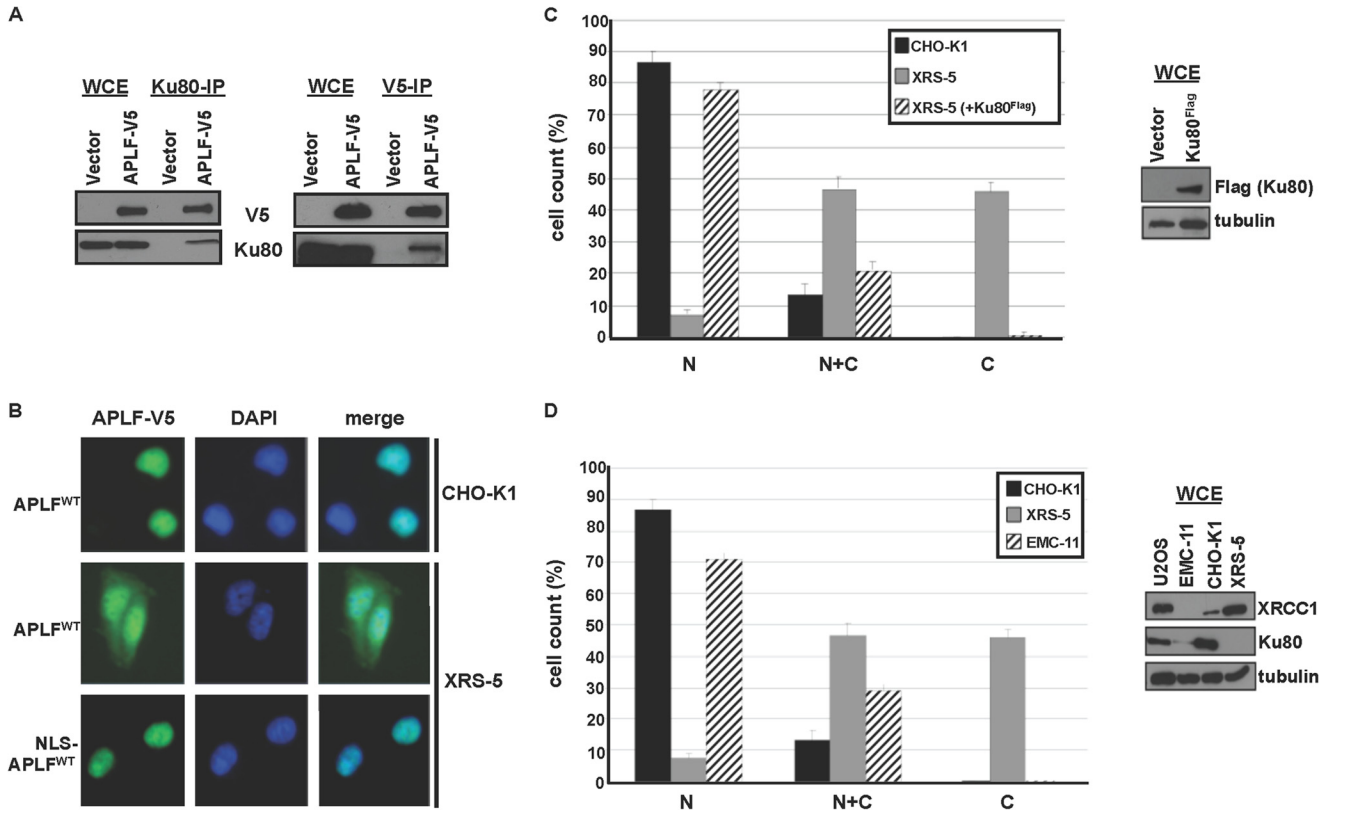

FIGURE 3. **Ku expression rescues APLF nuclear localization in Ku-deficient mammalian cells.** *A*, WCEs from CHO-K1 cells ectopically transfected with empty vector or APLF-V5 were immunoprecipitated with either anti-V5 or anti-Ku80 antibodies and immunoblotted with anti-Ku80 or anti-V5 antibodies as indicated. *B*, CHO-K1 and XRS-5 (Ku80-deficient) cells were transfected with V5-tagged APLF^{WT} or NLS-APLF^{WT} (XRS-5 cells), fixed, and immunostained with anti-V5 and DAPI, and images were merged (*right panels*). *C*, CHO-K1, XRS-5 and XRS-5 cells complemented with wild-type Ku80 (+Ku80^{Flag}) ectopically expressing APLF-V5 were fixed and immunostained with anti-V5 antibody, and the subcellular localization of APLF-V5 was quantified by immunofluorescence microscopy (as indicated in the legend for Fig. 2*D*). Ku80 expression in XRS-5 cells was confirmed by anti-Ku80 immunoblotting (*inset*, *lower panel*). *D*, CHO-K1, XRS-5, and EMC-11 (XRCC1-deficient) CHO cells ectopically expressing APLF-V5 were fixed, immunostained with anti-V5 antibody, and quantified by immunofluorescence microscopy (as indicated in the legend for Fig. 2*D*). *Inset*, WCEs were immunoblotted with antibodies as indicated along with WCEs from human U2OS cells as a control.

the co-expression of human Ku80 (Ku80^{Flag}) with WT APLF-V5 in XRS-5 cells was associated with a dramatic increase in the nuclear retention of WT-APLF compared with XRS-5 cells expressing only WT-APLF and was similar to the cellular phenotype observed when WT APLF was examined in the CHO-K1 cells (Fig. 3*C*).

As another control, we next examined PNKP and APTX, both of which interact with XRCC4-ligase IV, but not with Ku, and which both possess classical NLS. When expressed in either wild-type CHO-K1 or XRS-5 cells, both PNKP-V5 and APTX-V5 were entirely nuclear (supplemental Fig. S2). Furthermore, human APLF-V5 expressed in XRCC4-deficient XR-1 or DNA-PKcs-deficient XRC-1 CHO cell lines exhibited a subcellular distribution similar to that observed when APLF-V5 was expressed in CHO-K1 cells (supplemental Fig. S3*A*). Therefore, the subcellular localization of APLF does not appear to depend on XRCC4 or DNA-PKcs.

A previous report has suggested that XRCC1 is important for the subcellular localization of APLF (20). When we examined the subcellular localization of APLF in the XRCC1-deficient CHO cell line EMC-11, we did observe a decrease in the nuclear retention of APLF-V5 compared with that observed in the CHO-K1 cells (Fig. 3*D*), but this was not as great as the defect observed in the XRS-5 cells. To further investigate this result, we examined the various CHO cells lines for the expression of XRCC1 and Ku80. As expected, the XRS-5 cell line expressed XRCC1 but no detectable Ku80. In the XRCC1-deficient cell line, EMC-11, XRCC1 was not detected as expected, but to our surprise Ku80 levels were diminished compared with those in CHO-K1 cells (Fig. 3*D*). Therefore, XRCC1 expression does not appear to correlate with APLF subcellular localization, but the diminished Ku80 levels in the XRCC1-deficient cell line may explain why APLF subcellular localization was altered. This idea is consistent with our observation that the expression of the APLF FHA mutant, R27A, which disrupts phosphothreonine-dependent interactions with XRCC1 and XRCC4, did not exhibit defective subcellular location in U2OS cells (supplemental Fig. S3*B*). Lastly, the subcellular localization of WT APLF or the deletion mutant APLF$^{\Delta 180-200}$-V5 in U2OS cells was unaffected following exposure to γ-IR (supplemental Fig. S4).

The C-terminal Region of Ku80 Is Not Required for Interactions with APLF—Although Ku80 is highly homologous to Ku70, the C-terminal region of Ku80 is divergent and has been shown to be required for cellular radioresistance (30). This region of Ku80 is also required for DNA-PKcs autophosphorylation and activation of Artemis end processing (30). Therefore, we questioned whether this C-terminal portion of Ku80 might

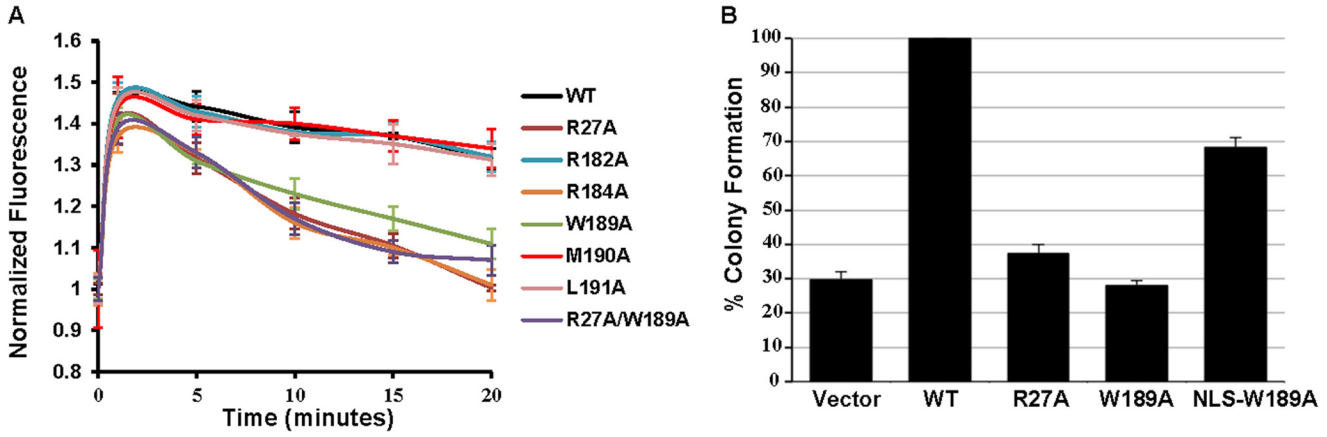

FIGURE 4. **The FHA domain and Ku-binding motif are required for APLF assembly at sites of DNA damage and for APLF-dependent NHEJ.** *A*, U2OS cells stably depleted of endogenous APLF (U2OS^{KD}) and ectopically expressing RNAi-resistant and eGFP-tagged APLF^{WT}, APLF^{R27A}, APLF^{W189A}, APLF$^{R27A/W189A}$, APLF^{R182A}, APLF^{R184A}, APLF^{M190A}, or APLF^{L191A} were subjected to two-photon laser micro-irradiation, and recruitment to the laser tracks was visualized and quantified over a 20-min period. At least 10 cells were quantified per sample. *Error bars* represent S.E. *B*, U2OS^{KD} cells were transfected with empty vector, RNAi-resistant APLF^{WT}, APLF^{R27A}, APLF^{W189A}, or NLS-APLF^{W189A} and then transfected with linearized plasmid DNA containing a puromycin resistance cassette 48 h later and replated in triplicate at low density in media containing puromycin 24 h later. The resulting puromycin-resistant colonies were stained and quantified 10 days later. The relative plasmid integration with RNAi-resistant APLF^{WT} was set at 100% integration. The data were derived from three independent experiments performed in triplicate. *Error bars* represent the S.D.

be important for directing interactions with APLF. To this end, XRS-5 cells were reconstituted with WT-Ku80 or Ku80$^{1-569}$ missing these C-terminal sequences of Ku80. The cell extracts were then examined in pulldown assays with immobilized GST-APLF and immunoblotted for Ku80 (and Ku70 as a control). We found that the expression of EGFP-tagged Ku80^{WT} or Ku80$^{1-569}$ restored Ku70 levels in the XRS-5 cells as expected (supplemental Fig. S5*A*). Furthermore, under these conditions GST-APLF interacted equally well with both Ku80^{WT} and the truncated mutant protein, Ku80$^{1-569}$, suggesting that the C-terminal residues of Ku80 are not required for interaction with APLF. Lastly, both Ku80^{WT} and Ku80$^{1-569}$ effectively restored the predominantly nuclear localization of WT-APLF expressed in XRS-5 cells (supplemental Fig. S5*B*).

The Interaction of APLF with Ku and XRCC4 Facilitates the Assembly of APLF at Sites of DNA Damage and NHEJ—We have previously shown that the APLF PBZ domains are involved in the initial recruitment of APLF to sites of laser-induced DNA damage (27). Whether Ku might also participate in the recruitment and assembly of APLF to sites of DSBs was not clear from the outset of these studies. APLF itself appears to enhance the retention of XRCC4 at sites of laser-generated DNA damage (31), suggesting that the assembly of APLF at sites of DNA damage is important for DSB repair. Therefore, it is possible that interactions with Ku and/or XRCC4 might stabilize APLF at sites of DNA damage. To investigate this further, we examined APLF retention at sites of laser-induced DNA damage over a 20-min time period. U2OS cells stably depleted of endogenous APLF by shRNA were reconstituted with RNAi-resistant EGFP-tagged WT APLF, APLF^{R27A}, APLF^{W189A}, and APLF$^{R27A/W189A}$, as well as the other Ku-binding mutants, and were subjected to laser micro-irradiation; recruitment kinetics were monitored over 20 min (Fig. 4*A* and supplemental Fig. S6). Overall, the assembly of APLF at the laser tracks was considerably reduced when the FHA domain, or the ability to interact with Ku80, was disrupted (Fig. 4*A*). The APLF^{R182A}, APLF^{M190A}, and APLF^{L191A} mutant proteins, which did not abolish interactions with Ku80, were the least affected in that the monitored assembly of these proteins over 20 min was similar to WT APLF (Fig. 4*A*). The recruitment kinetics of the APLF^{R184A} and APLF^{W189A} mutant proteins were similar to APLF^{R27A} and APLF$^{R27A/W189A}$, demonstrating decreased retention at sites of laser-induced DNA damage compared with WT APLF. In contrast, the immediate recruitment of these mutant proteins appeared similar to WT APLF (Fig. 4*A*).

We next wondered whether the APLF^{R27A} and Ku-binding mutant proteins might also be defective in DSB repair. Therefore, we next examined the role of the APLF-XRCC4 and APLF-Ku interactions in NHEJ using the random plasmid integration assay, which is dependent on NHEJ. APLF has been shown previously to be required for the random plasmid integration of a linearized plasmid DNA substrate in U2OS cells (18). Thus U2OS cells stably depleted of endogenous APLF by shRNA were transfected with RNAi-resistant V5-tagged APLF^{WT}, APLF^{R27A}, APLF^{W189A}, or NLS-APLF^{W189A} and examined for plasmid integration. As shown in Fig. 4*B*, the mutant APLF proteins with defective binding to the NHEJ components XRCC4-ligase IV (R27A and W189A) had the greatest reduction in relative colony formation compared with cells reconstituted with APLF^{WT}. Interestingly, the introduction of an NLS to the Ku-binding mutant APLF^{W189A} (NLS-APLF^{W189A}), which restores APLF nuclear retention and XRCC4 interaction, demonstrated a reduction in relative plasmid integration but was not as severely affected as the R27A or W189A mutant APLF proteins (Fig. 4*B*).

DISCUSSION

The APLF-Ku interaction is likely important for the function of APLF in NHEJ, and we sought to better understand the mechanism of this interaction. The results presented show that the Ku-binding motif on APLF localizes to a region between the FHA and tandem PBZ domains. The importance of this amino acid region is highlighted by the fact that it is evolutionarily conserved within APLF vertebrate homologues, and indeed,

deletion of this region on APLF resulted in diminished APLF-Ku interactions. A recent report has similarly found that this region of APLF is critical for the interaction with Ku (32). Moreover, and surprisingly, APLF nuclear retention was altered, with an increased redistribution of APLF to the cytoplasm in mammalian cells, either when the Ku-binding motif was disrupted or when WT human APLF was expressed in Ku-deficient mammalian CHO cells. APLF nuclear localization was rescued either upon reconstitution with Ku in the Ku-deficient cells or upon addition of an NLS onto APLF.

The APLF interaction with Ku was further defined to be strongly dependent on APLF amino acid residues Arg-184 and Trp-189, which are both invariant in mammalian APLF homologues. Substitution of either one of these residues resulted in the loss of an interaction with Ku and a dramatic reduction of APLF nuclear retention (Fig. 2*D*). Although other residues contained within the Ku-binding region, such as Arg-182 and Met-190, may contribute to the interaction with Ku, substitution of these residues resulted in a less severe effect on both Ku binding and APLF nuclear retention. A peptide corresponding to the APLF Ku-binding region was found to be sufficient to direct interactions with purified recombinant Ku heterodimer *in vitro*, suggesting that the APLF Ku-binding region might represent a general Ku-binding motif.

Consistent with the idea of a specific Ku-binding motif, other previously mapped Ku-binding regions for WRN and XLF possess amino acid sequence similarities to the APLF Ku-binding motif (33, 34), and peptides derived from these sequences were found to bind directly to Ku *in vitro* (Fig. 1*D*). Interestingly, the Ku-binding region of XLF, located at the extreme C terminus of the protein, has been shown to be required for the assembly of XLF at DSBs, and disruption of this region also reduces the association with XRCC4 (34). In addition, in both WRN and XLF the Ku-binding regions lie very close or overlap with their NLS. Indeed, in patients with Werner syndrome all of the mutations identified to date result in C-terminally truncated proteins lacking the NLS (35). These truncated WRN proteins are often undetectable when cell lines from Werner syndrome patients are examined, suggesting that the truncated proteins are unstable and rapidly degraded in the cytoplasm. Patients with XLF mutations have also been noted to have C-terminally truncated proteins, which also results in the cytoplasmic redistribution of the mutant proteins (15). Therefore, although it is not clear why these sequences overlap, the functional consequence of disrupting the Ku-binding region in WRN and XLF also impacts on subcellular localization and is relevant in human disease.

The site of XLF interaction on Ku has been suggested to localize to the N-terminal region of Ku (34). As was the case with APLF, the C-terminal region of Ku80 was found to be nonessential for the interaction with XLF (34). The existing data in the literature suggest that APLF interacts with Ku80 (19), likely via the Ku80 von Willebrand A domain (32). Whether APLF and XLF interact with the same or a different region of Ku requires further investigation.

At least one way that Ku appears to affect APLF function in DSB repair is by promoting its nuclear retention and association with XRCC4. APLF does not possess a classical NLS, and it is conceivable that APLF may be co-imported with Ku into the nucleus via the classical nuclear transport pathway. However, it is not clear what proportion of endogenous Ku complexes with APLF under basal conditions and whether the entire proportion of these complexes is important for mediating the nuclear localization of APLF. Furthermore, we cannot exclude the possibility that APLF may also be able to passively diffuse into the nucleus from the cytoplasm. Indeed, our results demonstrated that a small proportion of APLF is localized to the nucleus in Ku-deficient hamster cells under basal conditions, suggesting that APLF may be able to passively diffuse into the nucleus even in the absence of Ku. Overall, our data are consistent with APLF being engaged in basal interactions with Ku, which may both stabilize APLF and contribute to its nuclear retention. There are other reported examples of small molecular weight and NLS-deficient repair proteins that rely primarily on interactions with NLS-containing proteins, which are involved in their respective repair pathway, to bring them into the nucleus, often in a DNA damage-dependent manner (36, 37). This may represent a level of spatiotemporal regulation that is more efficient than simple diffusion.

The first 200 amino acid residues of APLF, which direct interactions with XRCC4-ligase IV and Ku but lack the C-terminal PBZ domains did not impair APLF nuclear localization under basal conditions, suggesting that the PBZ domains are not required for nuclear retention under these conditions. Furthermore, the highly conserved N-terminal FHA domain was not essential for the nuclear retention of APLF as monitored in CHO-K1 cells (supplemental Fig. S3). It remains possible, as reported previously, that FHA-mediated interaction with XRCC1 may facilitate APLF nuclear import/retention following exposure to specific forms of DNA damage such as hydrogen peroxide treatment (20). In contrast, following IR there was no substantial effect on the nuclear localization of APLF in the presence or absence of the Ku-binding motif (supplemental Fig. S4).

The initial recruitment of APLF to sites of DNA damage is PBZ- and poly(ADP-ribose)-dependent (27), but the retention of APLF at sites of DSBs appears to rely at least in part on additional protein-protein interactions with Ku and XRCC4. Indeed, the disruption of the APLF-XRCC4 ($APLF^{R27A}$) and APLF-Ku ($APLF^{R184A}$ and $APLF^{W189A}$) interactions impaired the assembly of APLF at sites of laser-generated DNA damage. These data are consistent with those from a recent report, which further demonstrate a requirement for the APLF-Ku interaction in the assembly of XRCC4 at laser tracks (32).

APLF-dependent NHEJ was also deleteriously affected by the disruption of the FHA domain ($APLF^{R27A}$) and Ku-binding motif ($APLF^{W189A}$). Interestingly, the measured effects of these APLF mutant proteins on APLF-dependent NHEJ appeared to be more marked than their effects on APLF recruitment, with these mutants having similar levels of plasmid integration as those seen with cells depleted of APLF (Fig. 4*B*). In contrast, $APLF^{R27A}$ and $APLF^{W189A}$ did not abolish APLF recruitment (Fig. 4*A*). This observation may be explained by the different types of DNA damage present in the two assays. Only linearized plasmid DNA (DSBs) was utilized in the plasmid integration assay, which would enhance the dependence of APLF on the

NHEJ factors, XRCC4 and Ku, for integration. In contrast, laser micro-irradiation would be expected to generate DNA damage consisting of SSBs and other forms of DNA damage, in addition to DSBs (38). This notion is consistent with the recent report showing an increased reliance on APLF-Ku interactions for APLF recruitment with increased energy output at the laser tracks (expected to generate increased DSBs) (32).

The disruption of the APLF Ku-binding motif impacted on the association with XRCC4, unless an NLS was introduced, suggesting that the APLF-Ku interaction at DSBs facilitates the subsequent interaction with XRCC4. This is consistent with the higher relative percentage of colony formation in U2OS cells expressing NLS-APLF^{W189A}, which rescues the association with XRCC4 (supplemental Fig. S1*B*) compared with APLF^{W189A} (Fig. 4*B*). We believe that this defect in XRCC4 association would not be evident unless examined in a cellular context, which could explain why recombinant XRCC4 and APLF Ku-binding mutant proteins have been reported to interact *in vitro* with no observable reduction (32). The deletion of the XLF Ku-binding motif similarly impairs XLF-XRCC4 interactions (34). These data identify a Ku-binding motif and suggest that the interaction of these NHEJ proteins, XLF and APLF, with Ku is important for their interaction with and assembly of XRCC4 at DSBs. Collectively, the results are consistent with initial PBZ-dependent binding of APLF to poly(ADP-ribose) at sites of DNA damage followed by an association with Ku that retains APLF at DSBs and promotes the interaction with XRCC4-ligase IV and thereby DNA end joining.

Acknowledgment—We thank the Advanced Optical Microscopy Facility at the Ontario Cancer Institute (University Health Network) for support with live cell imaging analyses.

REFERENCES

1. Jackson, S. P., and Bartek, J. (2009) The DNA damage response in human biology and disease. *Nature* **461,** 1071–1078
2. Polo, S. E., and Jackson, S. P. (2011) Dynamics of DNA damage response proteins at DNA breaks: a focus on protein modifications. *Genes Dev.* **25,** 409–433
3. Kass, E. M., and Jasin, M. (2010) Collaboration and competition between DNA double-strand break repair pathways. *FEBS Lett.* **584,** 3703–3708
4. Weterings, E., and van Gent, D. C. (2004) The mechanism of non-homologous end-joining: a synopsis of synapsis. *DNA Repair* **3,** 1425–1435
5. Koike, M. (2002) Dimerization, translocation and localization of Ku70 and Ku80 proteins. *J. Radiat. Res.* **43,** 223–236
6. Gell, D., and Jackson, S. P. (1999) Mapping of protein-protein interactions within the DNA-dependent protein kinase complex. *Nucleic Acids Res.* **27,** 3494–3502
7. Downs, J. A., and Jackson, S. P. (2004) A means to a DNA end: the many roles of Ku. *Nat. Rev. Mol. Cell Biol.* **5,** 367–378
8. Wu, X., and Lieber, M. R. (1996) Protein-protein and protein-DNA interaction regions within the DNA end-binding protein Ku70-Ku86. *Mol. Cell. Biol.* **16,** 5186–5193
9. Li, B., and Comai, L. (2002) Displacement of DNA-PKcs from DNA ends by the Werner syndrome protein. *Nucleic Acids Res.* **30,** 3653–3661
10. Yannone, S. M., Roy, S., Chan, D. W., Murphy, M. B., Huang, S., Campisi, J., and Chen, D. J. (2001) Werner syndrome protein is regulated and phosphorylated by DNA-dependent protein kinase. *J. Biol. Chem.* **276,** 38242–38248
11. Li, B., and Comai, L. (2001) Requirements for the nucleolytic processing of DNA ends by the Werner syndrome protein-Ku70/80 complex. *J. Biol. Chem.* **276,** 9896–9902
12. Ramsden, D. A., and Gellert, M. (1998) Ku protein stimulates DNA end joining by mammalian DNA ligases: a direct role for Ku in repair of DNA double-strand breaks. *EMBO J.* **17,** 609–614
13. Nick McElhinny, S. A., Snowden, C. M., McCarville, J., and Ramsden, D. A. (2000) Ku recruits the XRCC4-ligase IV complex to DNA ends. *Mol. Cell. Biol.* **20,** 2996–3003
14. Chen, L., Trujillo, K., Sung, P., and Tomkinson, A. E. (2000) Interactions of the DNA ligase IV-XRCC4 complex with DNA ends and the DNA-dependent protein kinase. *J. Biol. Chem.* **275,** 26196–26205
15. Ahnesorg, P., Smith, P., and Jackson, S. P. (2006) XLF interacts with the XRCC4-DNA ligase IV complex to promote DNA nonhomologous end-joining. *Cell* **124,** 301–313
16. Buck, D., Malivert, L., de Chasseval, R., Barraud, A., Fondanèche, M. C., Sanal, O., Plebani, A., Stéphan, J. L., Hufnagel, M., le Deist, F., Fischer, A., Durandy A., de Villartay, J. P., and Revy, P.(2006) Cernunnos, a novel nonhomologous end-joining factor, is mutated in human immunodeficiency with microcephaly. *Cell* **124,** 287–299
17. Yano, K., Morotomi-Yano, K., Wang, S. Y., Uematsu, N., Lee, K. J., Asaithamby, A., Weterings, E., and Chen, D. J. (2008) Ku recruits XLF to DNA double-strand breaks. *EMBO Rep.* **9,** 91–96
18. Macrae, C. J., McCulloch, R. D., Ylanko, J., Durocher, D., and Koch, C. A. (2008) APLF (C2orf13) facilitates nonhomologous end-joining and undergoes ATM-dependent hyperphosphorylation following ionizing radiation. *DNA Repair* (*Amst.*) **7,** 292–302
19. Kanno, S., Kuzuoka, H., Sasao, S., Hong, Z., Lan, L., Nakajima, S., and Yasui, A. (2007) A novel human AP endonuclease with conserved zinc-finger-like motifs involved in DNA strand break responses. *EMBO J.* **26,** 2094–2103
20. Iles, N., Rulten, S., El-Khamisy, S. F., and Caldecott, K. W. (2007) APLF (C2orf13) is a novel human protein involved in the cellular response to chromosomal DNA strand breaks. *Mol. Cell. Biol.* **27,** 3793–3803
21. Bekker-Jensen, S., Fugger, K., Danielsen, J. R., Gromova, I., Sehested, M., Celis, J., Bartek, J., Lukas, J., and Mailand, N. (2007) Human Xip1 (C2orf13) is a novel regulator of cellular responses to DNA strand breaks. *J. Biol. Chem.* **282,** 19638–19643
22. Caldecott, K. W. (2003) DNA single-strand break repair and spinocerebellar ataxia. *Cell* **112,** 7–10
23. Koch, C. A., Agyei, R., Galicia, S., Metalnikov, P., O'Donnell, P., Starostine, A., Weinfeld, M., and Durocher, D. (2004) Xrcc4 physically links DNA end processing by polynucleotide kinase to DNA ligation by DNA ligase IV. *EMBO J.* **23,** 3874–3885
24. Bernstein, N. K., Williams, R. S., Rakovszky, M. L., Cui, D., Green, R., Karimi-Busheri, F., Mani, R. S., Galicia, S., Koch, C. A., Cass, C. E., Durocher, D., Weinfeld, M., and Glover, J. N.(2005) The molecular architecture of the mammalian DNA repair enzyme, polynucleotide kinase. *Mol. Cell* **17,** 657–670
25. Ahel, I., Ahel, D., Matsusaka, T., Clark, A. J., Pines, J., Boulton, S. J., and West, S. C. (2008) Poly(ADP-ribose)-binding zinc finger motifs in DNA repair/checkpoint proteins. *Nature* **451,** 81–85
26. Rulten, S. L., Cortes-Ledesma, F., Guo, L., Iles, N. J., and Caldecott, K. W. (2008) APLF (C2orf13) is a novel component of poly(ADP-ribose) signaling in mammalian cells. *Mol. Cell. Biol.* **28,** 4620–4628
27. Li, G. Y., McCulloch, R. D., Fenton, A. L., Cheung, M., Meng, L., Ikura, M., and Koch, C. A. (2010) Structure and identification of ADP-ribose recognition motifs of APLF and role in the DNA damage response. *Proc. Natl. Acad. Sci. U.S.A.* **107,** 9129–9134
28. Görlich, D. (1998) Transport into and out of the cell nucleus. *EMBO J.* **17,** 2721–2727
29. Wagstaff, K. M., and Jans, D. A. (2009) Importins and beyond: non-conventional nuclear transport mechanisms. *Traffic* **10,** 1188–1198
30. Weterings, E., Verkaik, N. S., Keijzers, G., Florea, B. I., Wang, S. Y., Ortega, L. G., Uematsu, N., Chen, D. J., and van Gent, D. C. (2009) The Ku80 terminus stimulates joining and artemis-mediated processing of DNA ends. *Mol. Cell. Biol.* **29,** 1134–1142
31. Rulten, S. L., Fisher, A. E., Robert, I., Zuma, M. C., Rouleau, M., Ju, L., Poirier, G., Reina-San-Martin, B., and Caldecott, K. W. (2011) PARP-3 and APLF function together to accelerate nonhomologous end-joining. *Mol.*

Cell **41,** 33–45
32. Grundy, G. J., Rulten, S. L., Zeng, Z., Arribas-Bosacoma, R., Iles, N., Manley, K., Oliver, A., and Caldecott, K. W. (2013) APLF promotes the assembly and activity of non-homologous end joining protein complexes. *EMBO J.* **32,** 112–125
33. Karmakar, P., Snowden, C. M., Ramsden, D. A., and Bohr, V. A. (2002) Ku heterodimer binds to both ends of the Werner protein and functional interaction occurs at the Werner N terminus. *Nucleic Acids Res.* **30,** 3583–3591
34. Yano, K., Morotomi-Yano, K., Lee, K. J., and Chen, D. J. (2011) Functional significance of the interaction with Ku in DNA double-strand break recognition of XLF. *FEBS Lett.* **585,** 841–846
35. Comai, L., and Li, B. (2004) The Werner syndrome protein at the crossroads of DNA repair and apoptosis. *Mech. Ageing Dev.* **125,** 521–528
36. Santagati, F., Botta, E., Stefanini, M., and Pedrini, A. M. (2001) Different dynamics in nuclear entry of subunits of the repair/transcription factor TFIIH. *Nucleic Acids Res.***29,** 1574–1581
37. Knudsen, N. Ø., Andersen, S. D., Lützen, A., Nielsen, F. C., and Rasmussen, L. J. (2009) Nuclear translocation contributes to regulation of DNA excision repair activities. *DNA Repair* **8,** 682–689
38. Bekker-Jensen, S., Lukas, C., Kitagawa, R., Melander, F., Kastan, M. B., Bartek, J., and Lukas, J. (2006) Spatial organization of the mammalian genome surveillance machinery in response to DNA strand breaks. *J. Cell Biol.* **173,** 195–206